

Building nonstationary extreme value model using L-moments

Yire Shin¹, Yonggwan Shin^{2,*}, Jeong-Soo Park¹

1: Department of Statistics, Chonnam National University, Gwangju 61186, Korea

2: R&D center, XRAI Inc., Gwangju 61186, Korea

**: Corresponding author, email: syg.stat@gmail.com*

June 12, 2025

Abstract

The maximum likelihood estimation for a time-dependent nonstationary (NS) extreme value model is often too sensitive to influential observations, such as large values toward the end of a sample. Thus, alternative methods using L-moments have been developed in NS models to address this problem while retaining the advantages of the stationary L-moment method. However, one method using L-moments displays inferior performance compared to stationary estimation when the data exhibit a positive trend in variance. To address this problem, we propose a new algorithm for efficiently estimating the NS parameters. The proposed method combines L-moments and robust regression, using standardized residuals. A simulation study demonstrates that the proposed method overcomes the mentioned problem. The comparison is conducted using conventional and redefined return level estimates. An application to peak streamflow data in Trehafod in the UK illustrates the usefulness of the proposed method. Additionally, we extend the proposed method to a NS extreme value model in which physical covariates are employed as predictors. Furthermore, we consider a model selection criterion based on the cross-validated generalized L-moment distance as an alternative to the likelihood-based criteria.

Keywords: Cross-validated L-moment distance, Expected number of events, Solving nonlinear equations, Transformation to stationarity, Standard Gumbel distribution.

1 Introduction

The stationarity of time-series data is defined as a distribution that remains the same for any subsample of the original sample. However, natural phenomena rarely satisfy this hypothesis (Parey and Hoang 2021). In such cases, when a phenomenon evolves over time, a model-fitting technique that considers nonstationarity may be required.

Under stationarity, L-moment estimation (LME) often offers advantages over maximum likelihood estimation (MLE), including easy computation, robustness, and less bias for small and moderate sample sizes (Hosking and Wallis 1997; Jeong et al. 2014; Naghettini 2017). When estimating the shape parameter (ξ) and high quantiles of the generalized extreme value (GEV) distribution, LME outperforms MLE in terms of a lower root mean squared error (RMSE), especially when the upper endpoint is unbounded (Hosking et al. 1985; Yilmaz et al. 2021; Hossain et al. 2021).

Applying LME is not as straightforward in the case of nonstationarity or multivariate situations, whereas applying MLE is straightforward in complex situations. Therefore, MLE has been predominantly employed to estimate parameters of nonstationary (NS) extreme value models, which have recently received more attention in the context of climatic change (e.g., Konzen et al. 2021; Bousquet and Bernardara 2021; Choi 2021; Baldan et al. 2022; Prahadchai et al. 2023; Radfar et al. 2023). However, MLE is significantly influenced by outliers or large values toward the end of a sample, resulting in inferior performance in such cases.

Several studies have considered LME as a valuable and robust alternative to MLE to analyze time-dependent NS extreme values. Strupczewski and Kaczmarek (2001) considered the weighted least squares (WLS) method in which the parameters were estimated using the LME method for standardized residuals. However, the WLS estimator is sometimes too sensitively influenced by large values toward the end of a sample. Moreover, Ribereau et al. (2008) and Mudersbach and Jensen (2010) considered L-moment-based methods to analyze time-dependent NS extreme values, which are computationally easier but perform well only under restricted assumptions.

Gado and Nguyen (2016a) proposed a method (called GN16 hereafter) based on the framework by Cunderlik and Burn (2003). The GN16 method, which obtained stationary L-moment estimates for the detrended sequences, performs well in many cases for the NS GEV model, except for positive trends in the standard deviation.

This study focuses on developing a new algorithm to estimate NS parameters efficiently to overcome the weaknesses of the GN16 and WLS methods. The proposed method employs robust regression, transformation to stationary data, and LME. We expect the advantages of LME for a stationary model to continue to hold when estimating the parameters of NS models using the proposed method.

Section 2 describes extreme value models and preliminaries, and Section 3 presents the existing L-moment-based methods for NS GEV models and the proposed method. Next, Sections 4 and 5 provide a simulation study and a real data application. Section 6 extends the proposed method to the NS model with physical covariates. Finally, discussion and conclusion are provided in Sections 7 and 8. The accompanying Supplementary Information includes additional tables and figures.

2 Extreme value models and estimation

2.1 Generalized extreme value distribution

The GEV distribution (GEVD) has been widely used to model the extremes of natural phenomena and human society. The primary reason for applying GEVD is that it is supported by the large sample theory (Coles 2001). The cumulative distribution function (CDF) of the stationary GEVD is as follows (Hosking and Wallis 1997):

$$F(x) = \exp \left\{ - \left(1 - \xi \frac{x - \mu}{\sigma} \right)^{1/\xi} \right\}, \quad (1)$$

when $1 - \xi(x - \mu)/\sigma > 0$ and $\sigma > 0$, where μ , σ , and ξ are the location, scale, and shape parameters, respectively. The case of $\xi = 0$ in (1) corresponds to the Gumbel distribution. It is important to note that the sign of ξ in (1) was changed from that in the work by Coles (2001) to follow the work by Hosking and Wallis (1997). The reason why the sign of ξ is changed in this study is that considerably many reports and softwares (Asquith 2011) based on L-moments, especially in hydrology, have employed the changed sign of ξ . Consequently, we remark again that the GEV distribution has different tails according to the sign of the shape parameter ξ ; heavy tail when $\xi < 0$, exponential when $\xi \rightarrow 0$, and light or bounded when $\xi > 0$, where an opposite sign to Coles (2001) is used.

We use the following notation: $Z_t \sim GEV(\mu_t, \sigma_t, \xi_t)$, for the time-dependent NS GEV model. For example,

$$\mu_t = \mu_0 + \mu_1 \times t, \quad (2)$$

$$\sigma_t = \exp(\sigma_0 + \sigma_1 \times t), \quad (3)$$

where we set $t = \text{year} - t_0 + 1$, so that $t = 1, 2, \dots, n$, where t_0 is a starting year of the observations and n is the sample size. An exponential function in (3) is used to ensure that the positivity of σ is respected for all t . The shape parameters (ξ_t) are challenging to estimate precisely; modeling ξ as a function of time is typically unrealistic (Coles 2001, pp. 106; Katz 2013). The GEV model with the location and scale parameters represented by (2) and (3) under constant shape parameter is denoted as the GEV11 model.

Simpler models can be built with a constant scale parameter: $\sigma_t = \sigma_0$. The GEV model with the time-dependent location parameter (2) and constant scale parameter σ_0 is denoted as the GEV10 model in this study. When $\mu_t = \mu_0 + \mu_1 \times t + \mu_2 \times t^2$, under constant scale and shape parameters, the model is called the GEV20 model. Many other NS GEV models including the GEV11 and GEV20 models are considered in Coles (2001), Reiss and Thomas (2007), AghaKouchak et al. (2013), Katz (2013), and Prahadchai et al. (2023), for instance.

2.2 L-moment estimation

Hosking (1990) introduced L-moments as a linear combination of the expectations of order statistics. The r th L-moments (λ_r) of a probability distribution are defined as follows:

$$\lambda_1 = E(X_{1:1}), \quad \lambda_2 = \frac{1}{2}E(X_{2:2} - X_{1:2}), \quad \lambda_3 = \frac{1}{3}E(X_{3:3} - 2X_{2:3} + X_{1:3}), \quad (4)$$

$$\lambda_r = r^{-1} \sum_{j=0}^{r-1} (-1)^j \binom{r-1}{j} E(X_{r-j:r}), \quad r > 3, \quad (5)$$

where $X_{k:n}$ is the k th smallest observation from a sample of size n . The L-moment ratios are defined as follows: $\tau_2 = \lambda_2/\lambda_1$, $\tau_r = \lambda_r/\lambda_2$, $r = 3, 4, \dots$. The sample L-moments, denoted by l_r , were obtained as unbiased estimates of λ_r . Usually, l_r is a linear combination of the ordered sample values $x_{1:n}, \dots, x_{n:n}$. The sample L-moment ratios are obtained as follows: $t_2 = l_2/l_1$, $t_r = l_r/l_2$, $r = 3, 4, \dots$

Analogous to the usual method of moments estimation, the LME obtains parameter estimates by equating the first p sample L-moments to the corresponding population quantities. With small and moderate samples, the LME is often more efficient, robust, and computationally convenient than the MLE (Hosking et al. 1985; Naghettini 2017; Hossain et al. 2021).

2.3 Redefined return levels

The $1/p$ return level (RL) is defined as the $1-p$ quantile of the GEVD. For the annual extreme data, sometimes the name ‘‘T-year RL’’ is also used, with the ‘‘return period’’ $T = 1/p$. Various return levels are available for the NS model (Salas and Obeysekera 2014). In this study, two types of RLs are considered. The first is the conventional or ‘‘effective’’ RL (Katz 2013). The conventional T -year RL for the GEV model is defined as follows:

$$r_T^C(t) = \mu(t) - \frac{\sigma(t)}{\xi} \left[1 - y_T^{-\xi} \right], \quad \text{for } \xi \neq 0, \quad (6)$$

where $y_T = -\log(1 - 1/T)$. This RL is still useful but may not be sufficient to explain many aspects of the estimation of risk-related quantities for NS extreme data. Thus, the following so-called ‘redefined RLs’ are also considered in this study.

The redefined T -year RL (r_T^P) by Parey et al. (2010) is derived by relating the return period to the expected number of events, which is the solution of the following equation:

$$1 = \sum_{t=1}^T (1 - \hat{F}_t(r_T^P)), \quad (7)$$

where \hat{F}_t denotes the estimated CDF, as in (1), of the NS GEV model. The number 1 on the left side of (7) corresponds to the expected number of events exceeding r_T^P in T years (Salas et al. 2018). The redefined RL does not depend on time t but is a constant.

In a nonstationary context, no unique definition exists for the RL because extreme values recorded during the time $1, \dots, t$ have a different distribution than the extremes occurring during a different time $1 + C, \dots, t + C$ for any $C \neq 0$ (Ribereau et al. 2008). Olsen et al. (1998) defined another RL based on interpreting the return period as the expected waiting time. Here, return period T or the expected value of the waiting time until when the flood exceeds r_T for the first time is represented by the following equation (Cooley 2013; Salas et al. 2018):

$$T = 1 + \sum_{x=1}^{\infty} \prod_{t=1}^x F_t(r_T). \quad (8)$$

For computational practice, Cooley (2013) and Salas and Obeysekera (2014) recommended to use x_{max} which satisfies $F_t(x_{max}) = 1$, for the infinite summation. In this study, however, we did not employ this formula due to technical difficulties arising in solving the equation (8) related to the summation up to x_{max} .

3 L-moment-based algorithm for nonstationary GEV model

3.1 Weighted least squares

Strupczewski and Kaczmarek (2001) and Strupczewski et al. (2016) proposed the following WLS method for the GEV11 model:

- Step 1. Fit $Z_t = \mu_0 + \mu_1 \times t$ to the data using the least squares method to obtain $(\hat{\mu}_0, \hat{\mu}_1)$ or $\hat{\mu}_t = \hat{\mu}_0 + \hat{\mu}_1 \times t$.
- Step 2. Construct pseudo-residuals as follows: $\epsilon_t = Z_t - \hat{\mu}_t$.
- Step 3. Construct $\epsilon'_t = |\epsilon_t - \bar{\epsilon}|$, where $\bar{\epsilon}$ is the average of ϵ_t , and implement a regression method to fit $\sigma_t = \exp(\sigma_0 + \sigma_1 t)$ to ϵ'_t to obtain $(\hat{\sigma}_0, \hat{\sigma}_1)$ or $\hat{\sigma}_t = \exp(\hat{\sigma}_0 + \hat{\sigma}_1 t)$.
- Step 4. Find the WLS estimates $(\hat{\mu}_0, \hat{\mu}_1)$ that minimize $\sum_{t=1}^n (Z_t - (\mu_0 + \mu_1 \times t))^2 / \hat{\sigma}_t^2$.
- Step 5. Construct $Z'_t = [Z_t - (\hat{\mu}_0 + \hat{\mu}_1 \times t)] / \hat{\sigma}_t$.
- Step 6. Calculate the stationary LME $(\hat{\mu}_{st}, \hat{\sigma}_{st}, \hat{\xi}_{st})$ from $\{Z'_t\}$ based on the stationary GEVD.
- Step 7. Compute a quantile function of the NS model as follows:

$$X(q, t) = Y(q) \times \hat{\sigma}_t + (\hat{\mu}_0 + \hat{\mu}_1 \times t), \quad (9)$$

where $Y(q)$ is the quantile function (for $0 < q < 1$) obtained from a stationary GEVD with $(\hat{\mu}_{st}, \hat{\sigma}_{st}, \hat{\xi}_{st})$.

The main idea of WLS method is that it fits the data by a NS trend model firstly, and then it applies the stationary LME to the standardized residuals (representing irregular fluctuation around the trend) to obtain the final quantile estimate. The first part is consisted of using regression model to approximate an initial location parameter, stabilizing the detrended residuals to obtain useful weights and scale parameter, and estimating anew NS location parameter by the weighted regression. In the second part, the stationary LME is computed for the standardized residuals which are assumed to be independent and identically distributed. The final quantile estimates are obtained by combining the above first and scond components.

Step 7 is sufficient to calculate the conventional RL function. However, for further analysis such as testing hypothesis on a particular parameter or estimating the redefined RL by Parey et al. (2010), we need to obtain an estimate for each parameter. The details on obtaining them are presented in the Appendix.

3.2 Method by Gado and Nguyen (2016)

For the GEV11 model, the GN16 method applies the following algorithm, where Steps 1 to 3 are the same as those for the WLS method. Step 4 in the WLS method is no longer implemented; instead, the following algorithm is used:

- Step 5. Construct the following pseudo-residuals using the formula from Cunderlik and Burn (2003):

$$Q_t^{max} = \begin{cases} \epsilon_t - \text{sign}(\hat{\sigma}_t) \times \hat{\sigma}_t & \text{for } \epsilon_t \geq \bar{\epsilon} \\ \epsilon_t + \text{sign}(\hat{\sigma}_t) \times \hat{\sigma}_t & \text{for } \epsilon_t < \bar{\epsilon}, \end{cases} \quad (10)$$

where $\text{sign}(\hat{\sigma}_t) = +1$ or -1 accordingly when $\hat{\sigma}_t$ has an increasing or decreasing trend, respectively.

- Step 6. Calculate the stationary LMEs $(\hat{\mu}_{st}, \hat{\sigma}_{st}, \hat{\xi}_{st})$ from $\{Q_t^{max}\}$ based on the stationary GEVD.
- Step 7. Estimate the new NS parameters $(\hat{\mu}_0, \hat{\mu}_1, \hat{\sigma}_0, \hat{\sigma}_1, \hat{\xi})$ through the relationship between the GEV parameters and temporal moments, where $\hat{\xi} = \hat{\xi}_{st}$ (detailed in the GN16 method).

The NS parameter estimates by considering the relationship between GEV parameters and the temporal moments in Step 7 are

$$\hat{\mu}_t = \hat{\mu}'_0 + \hat{\mu}'_1 \times t - b(\hat{\xi}) \hat{\sigma}_t, \quad (11)$$

$$\log(\hat{\sigma}_t) = \hat{\sigma}'_0 + \log c(\hat{\xi}) + \hat{\sigma}'_1 \times t, \quad (12)$$

where

$$b(\hat{\xi}) = \frac{1 - \Gamma(1 + \hat{\xi}_{st})}{\hat{\xi}_{st}} \quad \text{and} \quad c(\hat{\xi}) = \left[\frac{\hat{\xi}_{st}^2}{\Gamma(1 + 2\hat{\xi}_{st}) - \Gamma^2(1 + \hat{\xi}_{st})} \right]^{1/2}.$$

In (11), $\hat{\mu}'_0, \hat{\mu}'_1, \hat{\sigma}'_0, \hat{\sigma}'_1$ are the estimates obtained in the Steps 1 to 3 of the WLS method. It is notable that only $\hat{\xi}_{st}$ among three stationary LMEs is used in the above formula.

The main idea of the GN16 method is similar to the WLS in the sense that both methods first estimate a trend component and then construct a residuals for which the stationary LME can be applied. Notably, the formula (Q_t^{max}) by Cunderlik and Burn (2003) in Step 5 for constructing pseudo-residuals is different from that (Z'_t) of the WLS method. However, the basic idea of constructing Q_t^{max} is similar to that of Z'_t of the WLS method in the sense that Z'_t and Q_t^{max} are the detrended and rescaled series. However, in the Step 7, the NS parameters are estimated differently from the WLS method.

Using this method, Gado and Nguyen (2016b) investigated the NS behavior of flood peaks in Quebec. The GN16 method performs better than MLE and stationary LME for most cases, except for the GEV11 model with positive trends in the standard deviation (GN16). Thus, in this study, the attempts to improve the GN16 method are focused on the GEV11 model with positive trends in the standard deviation.

One reason why the GN16 method did not work well for the case may be related to the stationarity of Q_t^{max} , in our opinion. We observed that $\hat{\sigma}'_0 = \hat{\sigma}_0 + \log c(\hat{\xi})$ in (11) is sometimes too small, which led to under-estimation of quantiles. This problem may be due to a biased estimation of $\hat{\xi}_{st}$ from Q_t^{max} which was not well constructed to be stationary. Another reason may be because the parameters are estimated once based on Q_t^{max} and never being updated, without checking the stationarity of Q_t^{max} . Thus the proposed method updates some estimates, which were obtained from the GN16 or WLS methods, to make the standardized residuals follow a stationary distribution very well. Another reason is because the GN16 method was heavily influenced by outliers or large values near the end of sample, which were observed in some of our experiments. In the GEV11 model with positive trends in the standard deviation, there was a tendency of showing more outliers toward the end of sample, which sometimes led the GN16 method to absurd fit.

3.3 Proposed method

In the above two methods, the NS sequence was transformed into independent and identically distributed random variables when applying the LME method, as in Step 5 of each method. For this proposal, after taking the similar steps as the Steps 1 and 3 of the WLS method, we considered a different transformation, \tilde{Z}_t , defined as follows:

$$\tilde{Z}_t = \frac{-1}{\hat{\xi}} \log \left\{ 1 - \hat{\xi} \frac{Z_t - \hat{\mu}_t}{\hat{\sigma}_t} \right\}. \quad (13)$$

Then, \tilde{Z}_t follows the standard Gumbel distribution, assuming the parameter estimates are true (Coles 2001, pp. 110). See the Supplementary Information for a proof that \tilde{Z}_t really follows the standard Gumbel distribution. \tilde{Z}_t is referred to as “standardized residuals.”

The proposed method refines the GN16 method as follows:

- Step 1. Obtain parameters $\hat{\mu}_0$, $\hat{\mu}_1$, $\hat{\sigma}_0$, $\hat{\sigma}_1$, $\hat{\xi}$ from the GN16 method, where a robust regression is used in Steps 1 and 3 of the WLS method.
- Step 2. Find μ_0 , σ_0 and ξ that satisfy the following system of three equations under the condition that $\hat{\mu}_1$, $\hat{\sigma}_1$ are fixed:

$$\lambda_1 = l_1(\tilde{Z}_t), \quad \lambda_2 = l_2(\tilde{Z}_t), \quad \tau_3 = t_3(\tilde{Z}_t), \quad (14)$$

where λ_1 , λ_2 , and τ_3 are the L-moments of a standard Gumbel distribution, and $l_1(\tilde{Z}_t)$, $l_2(\tilde{Z}_t)$, and $t_3(\tilde{Z}_t)$ are sample L-moments calculated from the transformed data $\{\tilde{Z}_t\}$.

In Step 1, an ordinary linear model was used in the WLS and GN16 methods for the GEV11 model, whereas Ribereau et al. (2008) recommended the application of a robust regression method. In addition, GN16 used Sen’s robust estimator for the GEV10 model. Thus, we employed a robust regression using the function `lmrob` in the ‘robustbase’ package in R (Koller and Stahel 2017). The robust regression used here is the MM-estimator derived by Yohai (1987), in which the regression parameters are estimated by determining the solution to $p + 1$ equations:

$$\sum_{i=1}^n \Psi(r_i/\hat{\tau})x_{ij} = 0, \quad j = 0, \dots, p, \quad (15)$$

where $x_{i0} = 1$, p denotes the number of independent variables, and r_i represents the residuals from the ordinary least squared estimation. Here, Ψ is the redescending influence function which down-weights the residuals that are far from zero. Moreover, $\hat{\tau}$ indicates a robust measure of variation based on the residuals. A popular choice of Ψ is Tukey’s biweight function (Wilcox, 2021). A usual selection of $\hat{\tau}$ is $1.4826 \{1 + 5/(n - p)\} \times \text{med}(|r_i|)$.

In Step 2, the transformation to $\{\tilde{Z}_t\}$ is a function of μ_0 , σ_0 and ξ ; that is,

$$\tilde{Z}_t = \tilde{Z}_t(\mu_0, \sigma_0, \xi \mid \hat{\mu}_1, \hat{\sigma}_1). \quad (16)$$

The population L-moments $(\lambda_1, \lambda_2, \tau_3)$ are obtained from the standard Gumbel distribution, where $\lambda_1 = 0.572215$ (the Euler constant), $\lambda_2 = \log(2)$, and $\tau_3 = 0.169925$.

The proposed method searches the estimates of $(\mu_0, \sigma_0, \text{ and } \xi)$ which make the standardized residuals $\{\tilde{Z}_t\}$ follow the standard Gumbel distribution as closely as possible in the L-moment sense. To solve a system of three equations in Step 2, we employed an iterative root-finding routine using the ‘`nleqslv`’ and ‘`lmomco`’ packages (Asquith, 2011) in R. The algorithm in ‘`nleqslv`’ package is based on Newton’s method for nonlinear equations for finding the roots of differentiable functions, that uses iterated local linearization of a function to approximate its roots. This algorithm is powerful and faster in general than other root-finding methods, but convergence is not guaranteed. Convergence depends on the initialization and behaviour of the

first derivatives in the neighborhood of a particular root (Dennis and Schnabel 1996). Thus we tried several (such as 20) starting values in our code with a limited number of iterations. When multiple solutions which satisfying (14) are found, we employed a goodness-of-fit criterion to choose the best among those multiple solutions, which is discussed in Section 7. When a solution satisfying (14) is not found, the proposed method uses the estimates obtained in the previous step. But the failure rate was less than 0.05% in our experiments.

In Step 2, the proposed algorithm fixes two coefficients ($\hat{\mu}_1$ and $\hat{\sigma}_1$) for the time variable and updates the other parameters (μ_0 , σ_0 , and ξ) that are not directly related to the time variable. The rationale for updating the other parameters is that those parameters may not be obtained well in the GN16 method. This rationale is used again in developing an estimation algorithm for a general NS GEV model with physical covariates, as described in Section 6.1.

3.4 Methods for GEV10 and GEV20 models

Methods for the GEV11 model presented in the previous sections can be similarly applied to the GEV10 and GEV20 models with some modifications. Because the scale parameter is constant in the GEV10 and GEV20 models, we did not require Step 3 in the WLS method. Moreover, $Q_t^{max} = \epsilon_t$ in Step 5 of the GN16 method. For GEV10, Sen's nonparametric robust estimators for μ_0 and μ_1 , as presented in the GN16 method, are employed in Step 1 in the WLS and GN16 methods. For GEV20, the regression coefficients (μ_0 , μ_1 , and μ_2) are estimated using a robust regression method.

4 Simulation study

4.1 Simulation setting

To evaluate the performance of the considered methods, we conducted a small Monte Carlo simulation study where RL is already known. The considered methods for comparison are MLE, stationary LME, WLS, the GN16 method, and the proposed method. We generated 1,000 random samples from the NS GEV11 model. In this simulation, we set μ_t and σ_t as in (2) and (3), with sample sizes of $n = 25$ and $n = 50$. For the parameters of GEV11, we first set $\mu_0 = 0$, $\mu_1 = -.1$, $\sigma_0 = 1$, and $\sigma_1 = .02$, following GN16, which is a decreasing location and increasing scale parameter setting as time changes. For the shape parameter, which is constant over time, we experimented with the following nine cases (in Hosking-Wallis notation): $\xi = -.35, -.25, -.15, -.05, 0.0, .05, .15, .25$, and $.35$. Note again that negative ξ stands for heavy tail, whereas positive ξ represents for light or bounded tail. The focus of interest in this study is the estimation of the T -year conventional and redefined RLs at the end of the sample. Specifically, we set $T = 100$ for the conventional RL ($r_T^C(t)$) and $T = 50$ for the redefined RL (r_T^P).

We calculated the following evaluation measures for the above quantities to compare the five estimators:

$$\text{Bias} = \bar{r}_T - r_T, \quad \text{SE} = \left[\frac{1}{N} \sum_{i=1}^N (\hat{r}_T(i) - \bar{r}_T)^2 \right]^{1/2}, \quad \text{RMSE} = (\text{Bias}^2 + \text{SE}^2)^{1/2}, \quad (17)$$

where SE denotes the standard error, r_T represents the true RL, $\hat{r}_T(i)$ is the RL estimate from the i th simulation sample, and \bar{r}_T is the average of N number of RLs, where N indicates the number of simulation samples ($N = 1,000$). A smaller value is preferred for these measures.

4.2 Simulation results for the GEV11 model

Tables 1 and 2 present the simulation results for the bias, SE, and RMSE for the NS GEV11 model computed using the five methods. The best performance is indicated in bold font. The true RLs at the bottom of Tables 1 and 2 were calculated from the formulas in (6) and (7), respectively, using the given parameter setting.

The proposed method performed best for $\xi \leq .15$ in terms of the RMSE. The MLE worked well for $\xi \geq .2$ in terms of the RMSE but worked poorly for $\xi \leq -.25$. The differences in the RMSE values among methods for $\xi \geq .15$ were relatively minimal compared to the actual values at the bottom of each table (see Figure 1 too). Notably, in Table 1, for the conventional RLs, the stationary LME has the lowest SE but the highest bias. In Table 2, for the redefined RL, the stationary LME had high values for the bias and SE. For the redefined RL, the WLS worked well for $\xi \leq -.30$. Table 1 reveals that the WLS method has a low bias but a high SE.

The Supplementary Information provides 40 sample plots of 50-year conventional RL estimates obtained using the five methods for the GEV11 model. The random samples were generated under the settings for which $\mu_0 = 0$, $\mu_1 = -.1$, $\sigma_0 = 1$, $\sigma_1 = .02$, and $\xi = -.2$. From these plots, with $n = 50$, we observe that the behaviors of the MLE, WLS, and proposed methods are similar to some degree. The proposed method rarely results in RL plots far from the true RL plot. MLE works well in general, except in a few cases where the MLE exhibits an extremely high bias at the end of a sample. The performance of WLS is between that of the proposed method and MLE.

The RL plots of the MLE or WLS methods for the GEV11 model occasionally display parabolic curves far from the true RL function, reflecting that outliers or large values toward the end of a sample significantly influence these methods. For the same data, the proposed method often exhibits the lowest absolute slope line. Thus, the proposed method for the GEV11 model may be resistant to influential observations or outliers.

The efficiency of the proposed method may be due to the effectiveness of LME and because the transformed values follow the standard Gumbel distribution as closely as possible. Although the WLS and GN16 methods also employ LME, the proposed method goes further

Table 1: Simulation results for the conventional 100-year return level at the end of the sample. The bias, standard error (SE), and root mean squared error (RMSE) for the nonstationary generalized extreme value (GEV11) model were computed using five methods, with a sample size of $n = 50$, as ξ changes from $-.35$ to $.35$.

Measure	Method	ξ								
		-0.35	-0.25	-0.15	-0.05	0.0	0.05	0.15	0.25	0.35
Bias	MLE	26.71	10.12	5.87	2.09	1.08	0.57	0.24	-0.75	-0.77
	LME	-30.26	-22.54	-16.41	-12.40	-10.51	-9.45	-7.17	-5.65	-4.20
	WLS	1.88	0.12	0.89	0.30	0.17	-0.11	0.64	0.17	0.52
	GN16	-9.00	-10.07	-7.62	-6.69	-6.53	-6.75	-5.37	-5.12	-4.43
	PROP	-14.41	-9.83	-5.19	-2.90	-1.13	-1.19	0.48	0.56	1.11
SE	MLE	185.0	51.84	26.97	17.73	15.34	12.17	8.40	4.92	3.40
	LME	24.17	16.24	10.46	6.97	5.25	4.51	3.04	2.03	1.52
	WLS	50.35	37.80	23.47	17.27	13.33	11.24	8.43	6.44	5.25
	GN16	55.83	34.04	22.58	15.52	11.98	9.30	6.85	4.94	3.72
	PROP	32.92	22.43	16.44	12.54	10.70	9.49	8.03	6.76	5.77
RMSE	MLE	186.9	52.82	27.61	17.85	15.38	12.19	8.41	4.98	3.49
	LME	38.73	27.78	19.46	14.22	11.75	10.47	7.78	6.00	4.47
	WLS	50.39	37.80	23.48	17.27	13.33	11.24	8.46	6.45	5.27
	GN16	56.56	35.50	23.83	16.91	13.64	11.49	8.71	7.12	5.78
	PROP	35.93	24.49	17.24	12.87	10.76	9.56	8.04	6.78	5.88
True return level		79.51	58.79	43.95	33.21	28.59	25.36	19.55	15.19	11.89

GN16: method by Gado and Nguyen (2016a), WLS: weighted least squares by Strupczewski and Kaczmarek (2001), LME: stationary L-moment estimation, PROP: proposed method, MLE: maximum likelihood estimation.

(after the GN16 method) by computing LME one more time in Step 2, minimizing the discrepancy in the sense of L-moments between the standardized residuals and standard Gumbel distribution. This additional computation may lead to a more accurate estimation. In the GEV11 model with positive trends in the standard deviation, there are a tendency of showing more outliers toward the end of sample. We believe that employing the robust regression in Step 1 and double usage of L-moments in the proposed method may prevent the fit being too sensitive to outliers.

Table 2: Same as Table 1 but for 50-year return level redefined by Parey et al. (2010).

Measure	Method	ξ								
		-0.35	-0.25	-0.15	-0.05	0.0	0.05	0.15	0.25	0.35
Bias	MLE	6.56	2.73	1.62	0.57	0.19	0.16	0.01	-0.26	-0.28
	LME	11.80	7.00	4.51	2.55	1.72	1.33	0.66	0.08	0.01
	WLS	0.44	0.51	0.99	0.75	0.69	0.74	0.90	0.71	0.81
	GN16	-2.14	-3.26	-3.31	-3.33	-2.81	-3.24	-2.74	-2.49	-1.99
	PROP	0.45	-0.29	0.04	0.00	0.20	0.27	0.63	0.62	0.83
SE	MLE	38.84	13.83	8.71	6.02	5.32	4.10	2.93	1.88	1.34
	LME	24.17	16.24	10.46	6.97	4.90	4.51	3.04	2.03	1.52
	WLS	14.37	10.90	7.63	5.89	5.66	3.93	3.04	2.47	2.08
	GN16	20.00	13.32	8.75	6.01	5.14	4.06	3.13	2.35	2.21
	PROP	15.26	10.11	7.07	4.92	4.24	3.52	2.88	2.46	2.19
RMSE	MLE	39.39	14.10	8.86	6.05	5.32	4.11	2.93	1.90	1.37
	LME	26.89	17.69	11.39	7.42	5.19	4.70	3.11	2.03	1.51
	WLS	14.38	10.91	7.69	5.71	5.70	4.00	3.18	2.57	2.24
	GN16	20.11	13.72	9.36	6.92	5.86	5.20	4.16	3.42	2.91
	PROP	15.27	10.11	7.07	4.92	4.25	3.53	2.94	2.53	2.34
True return level		37.44	29.24	23.02	18.25	16.47	14.58	11.71	9.46	7.66

4.3 Simulation of the GEV10 and GEV20 models

For the parameters of GEV10, we set $\mu_0 = 0$, $\mu_1 = -.2$, and $\sigma = 1$, following GN16. For the parameters of GEV20, we set $\mu_0 = 50$, $\mu_1 = -.02$, $\mu_2 = .06$, and $\sigma = 33$.

Simulation results for the GEV10 and GEV20 models for the sample sizes of $n = 25$ and $n = 50$ are presented in Table 3 for 100-year the conventional RLs at the end of the sample. These tables reveal that stationary LME often performs the worst among the five methods, except for the GEV10 model with $n = 25$. The GN16 method outperforms MLE and stationary LME for GEV20, consistent with the results of GN16. The proposed method and WLS perform similarly well and sometimes share the best rank.

For cases when ξ positive (light or bounded tail), for the GEV11, GEV10, and GEV20 models, it is hard to conclude which method performs the best; the MLE or WLS or proposed method work well for some cases. But it is notable that the absolute values of the RMSE for ξ positive are relatively smaller than those for ξ negative, as seen in Figure 1. Thus the choice of estimation method for ξ positive may be less critical than for ξ negative.

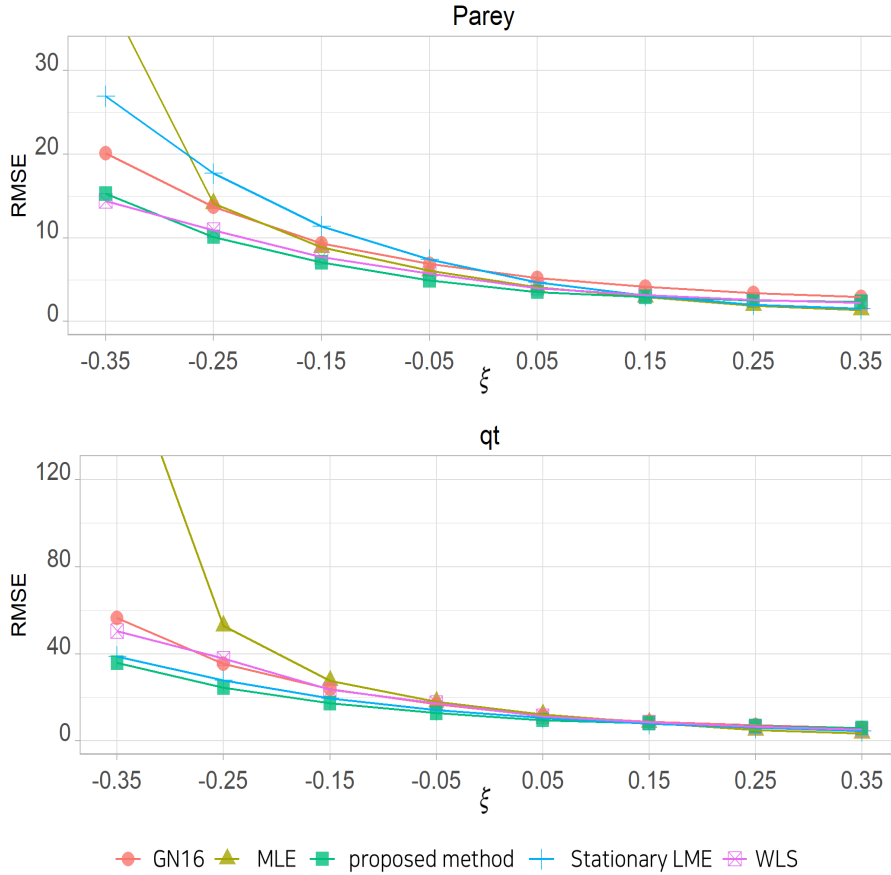


Figure 1: Simulation results: Root mean squared error (RMSE) of the 50-year return level (RL) redefined by Parey et al. (2010), the conventional 100-year RLs at the end of the sample (qt) from the GEV11 model fitted using the five methods, with a sample size of $n = 50$, as ξ changes from -0.35 to 0.35 . GN16: method by Gado and Nguyen (2016a), WLS: weighted least squares, MLE: maximum likelihood estimation.

5 Application: Peak streamflow in Trehafod

For an application, we considered the daily observed extreme flow data from the Rhondda River (Station ID:57006) in Trehafod in the UK. The dataset consists of peak flows from 1968 to 2021, spanning 54 years, with units in cubic meters per second (m^3/s).

Figure 2 displays a scatterplot of the data and the 50-year conventional RLs obtained from the GEV11 model fitted by the five methods. Among the four fitting methods, the WLS exhibited the steepest slope, whereas the proposed method had the least steep slope. Table 4 lists the parameter estimates and 50-year RL estimates.

Figure 3 illustrates the quantile-per-quantile (Q-Q) plots for the standardized residuals

Table 3: Simulation results for the root mean squared error of the conventional return levels at the end of the sample for the nonstationary GEV10 and GEV20 models with sample sizes of $n = 25$ and $n = 50$.

Model	n	Method	ξ								
			-0.35	-0.25	-0.15	-0.05	0.0	0.05	0.15	0.25	0.35
GEV10	25	MLE	12.1	9.8	6.7	5.5	4.6	3.9	3.4	2.7	1.9
		LME	11.7	8.3	5.3	4.6	4.4	4.0	3.9	3.9	3.8
		WLS	12.6	9.1	5.9	4.8	4.1	3.6	2.9	2.4	1.7
		GN16	12.7	10.0	7.6	6.0	5.0	4.6	3.9	3.5	2.8
		PROP	12.7	9.2	6.4	5.0	4.0	3.4	2.6	2.2	1.5
	50	MLE	10.0	7.1	5.6	4.1	3.5	2.9	1.8	1.3	1.0
		LME	9.6	7.1	6.3	5.9	6.1	6.0	6.1	6.7	7.3
		WLS	10.5	7.1	4.9	3.4	3.0	2.7	1.9	1.4	1.1
		GN16	10.5	9.0	6.9	5.8	4.9	4.6	3.6	3.1	2.7
		PROP	9.7	6.9	5.3	3.7	3.3	2.6	1.8	1.4	1.1
GEV20	25	MLE	22.5	18.4	16.8	13.7	10.9	9.6	8.3	6.6	5.5
		LME	25.3	18.0	13.1	9.8	8.6	7.7	6.8	6.7	6.3
		WLS	20.6	15.7	11.2	8.0	7.4	6.0	5.0	3.9	3.4
		GN16	21.2	16.7	13.0	9.5	7.9	7.5	6.3	6.0	5.3
		PROP	19.3	15.1	12.2	8.3	7.2	6.3	4.8	3.8	3.3
	50	MLE	21.7	17.6	16.0	13.2	10.8	9.4	8.0	6.4	5.1
		LME	20.7	18.0	13.0	9.5	8.7	7.5	6.4	6.3	5.9
		WLS	18.8	13.7	8.6	5.9	5.4	4.5	3.8	2.6	2.3
		GN16	20.0	16.5	11.5	8.7	7.6	7.0	6.2	5.0	4.6
		PROP	18.5	15.6	9.3	6.2	5.5	4.7	3.6	2.5	2.4

based on the five methods obtained from the GEV11 model. Two Q-Q plots for the stationary LME methods are remarkably similar because those parameter estimates are almost equal, as listed in Table 4. The Q-Q plots of the stationary LME method indicate that a discrepancy occurs in the upper end (one or two points). This discrepancy, especially at the upper end, reveals a significantly biased estimation of the high quantiles. The Q-Q plots for the proposed and MLE methods look better than those for other methods.

Table 5 and Figure 4 present the RL estimates and their plots based on the formula by Parey et al. (2010) obtained from the GEV11 model for the five methods. The RL plot in Figure 4 is a modified version of the usual RL plot in Coles (2001). This version is convenient to observe how the RL associated with the observations behaves as the return period changes up to 100 years. The four methods (MLE, stationary LME, WLS, and the proposed method)

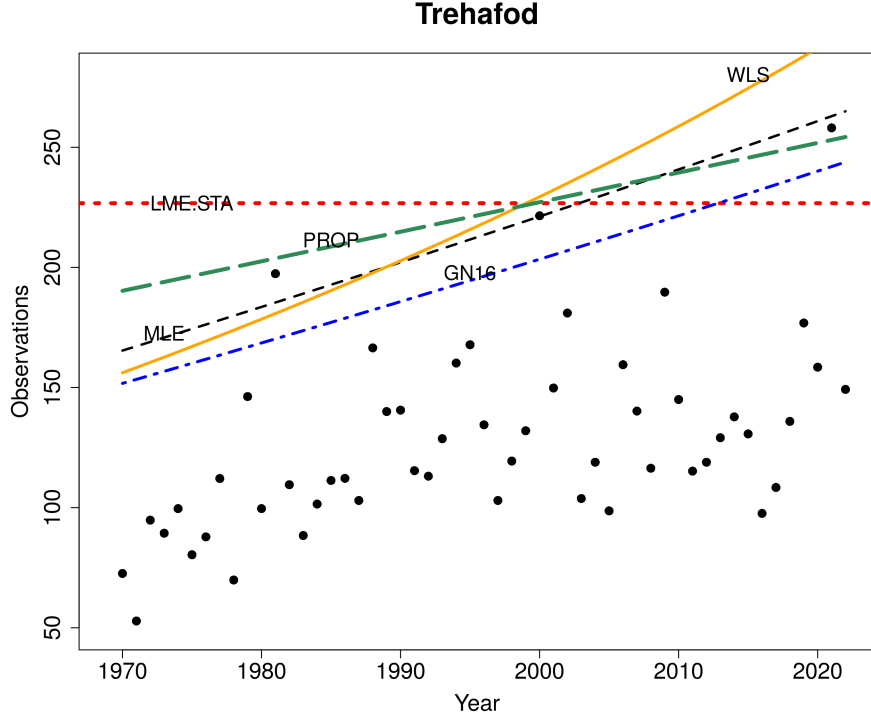


Figure 2: Scatterplot and 50-year conventional return levels for the GEV11 model fitted using several methods for extreme flow data (unit: m^3/s) in Trehafod, UK. GN16: method by Gado and Nguyen (2016a), PROP: proposed method, WLS: weighted least squares, LME.STA: stationary L-moment estimation, MLE: maximum likelihood estimation.

Table 4: Parameter estimates and 50-year return level estimates obtained from the GEV11 model using several methods for the extreme streamflow data in Trehafod, UK (unit: m^3/s).

Method	$\hat{\mu}_0$	$\hat{\mu}_1$	$\hat{\sigma}_0$	$\hat{\sigma}_1$	$\hat{\xi}$	r_T^P	$r_T^C(n)$
Gum.LME.STA	110.7		30.15			228.4	228.4
GEV.LME.STA	110.9		30.57		.015	226.7	226.7
MLE	81.3	1.19	2.99	.008	-.052	226.2	269.1
WLS	91.8	1.12	2.64	.016	-.063	233.9	298.2
PROP	82.9	1.09	3.12	.0013	-.093	225.1	254.3
GN16	89.6	1.20	2.64	.008	-.050	205.8	238.1

STA: stationary; r_T^P and $r_T^C(n)$ represent the return level estimates for $T = 50$ computed using the formula proposed by Parey et al. (2010) and the conventional method at $t = n$, respectively.

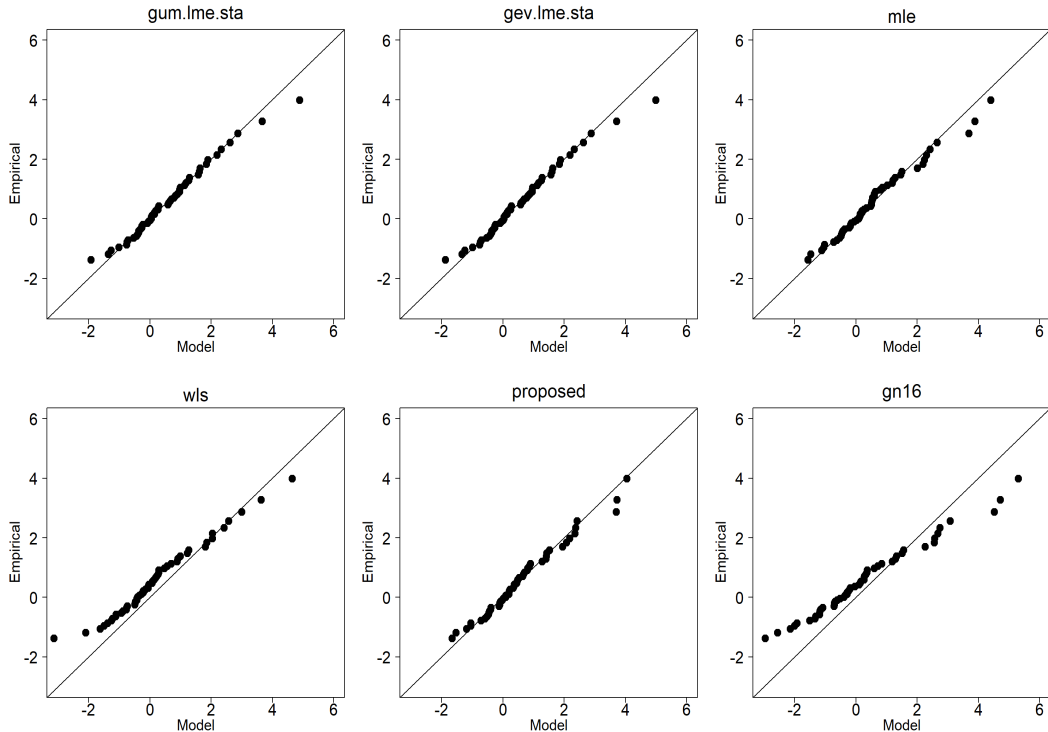


Figure 3: Quantile-per-quantile plots for standardized residuals based on the five methods, where the GEV11 model was fitted to the extreme streamflow data in Trehafod in the UK (unit: m^3/s).

have similar estimates at $T = 50$. For a return period longer than $T = 50$, the WLS provides the highest estimates, whereas the stationary LME provides the lowest estimates. For the stationary LME, it is unusual for the RL line to increase slowly for return periods longer than $T = 50$.

6 Extension and model selection based on L-moments

6.1 Extension to nonstationary model with physical covariates

One limitation of the proposed method is that only the time variable was employed as the covariate of the NS parameters. In this section, we extend the proposed method when covariates other than the time variable are included in the NS GEV model.

The NS GEV parameters can be written in the form: for example,

$$\mu(X) = \mu_0 + \mu_1 X_1 + \cdots + \mu_k X_k \quad (18)$$

$$\sigma(X) = \exp(\sigma_0 + \sigma_1 X_1 + \cdots + \sigma_k X_k), \quad (19)$$

Table 5: T -year return levels obtained using the formula by Parey et al. (2010) for several methods, where the GEV11 model was fit to the extreme streamflow data for Trehafod, UK (unit: m^3/s).

Method	Return level (T -year)					
	2	10	20	50	100	200
Gum.LME.STA	121.8	178.6	200.3	228.4	249.4	270.4
GEV.LME.STA	122.1	178.6	199.7	226.7	246.7	266.4
MLE	90.5	137.4	164.2	226.2	334.5	630.6
WLS	98.8	135.6	160.5	233.9	416.1	1471.9
PROP	92.9	146.0	173.4	225.1	293.1	422.5
GN16	96.6	131.5	152.8	205.8	299.9	549.1

Gum.LME.STA: stationary Gumbel distribution L-moment estimation, GEV.LME.STA: stationary generalized extreme value distribution L-moment estimation, MLE: maximum likelihood estimation, WLS: weighted least squares, PROP: proposed method, GN16: method by Gado and Nguyen (2016a).

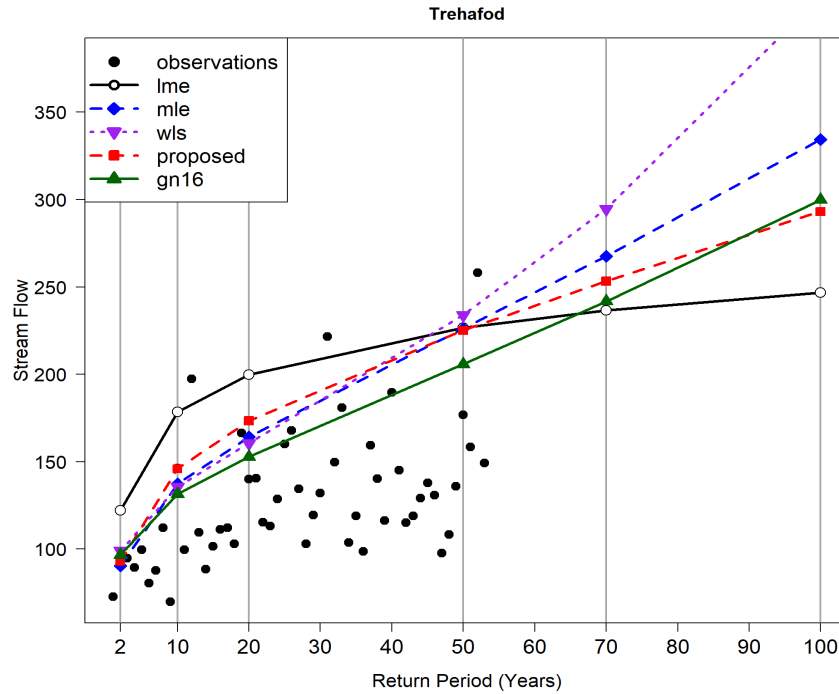


Figure 4: Modified return level plots based on the formula by Parey et al. (2010) for the five methods, where the GEV11 model was fit to the extreme streamflow data for Trehafod, UK (unit: m^3/s).

where X indicates a covariate vector and k is the number of covariates.

The central feature of the proposed method in the above sections was two steps. The first step was to estimate all parameters using a regression (the least squares or robust) method. The second step was to estimate the intercepts (μ_0 and σ_0) and the shape parameter ξ using stationary LME, fixing the estimates of other parameters. Applying this main feature similarly, we extend the proposed method to the NS GEV model in which physical covariates are employed as predictors. For an NS GEV model with $(\mu(X), \sigma(X), \xi)$, our extension is as follows:

- Step 1. Fit $Z_X = \mu_0 + \mu_1 X_1 + \dots + \mu_k X_k$ to the data using robust regression to obtain $(\hat{\mu}_0, \hat{\mu}_1, \dots, \hat{\mu}_k)$.
- Step 2. Construct absolute pseudo-residuals using $\epsilon_X = |Z_X - \hat{\mu}(X)|$.
- Step 3. Fit $\epsilon_X = \exp(\sigma_0 + \sigma_1 X_1 + \dots + \sigma_k X_k)$ using regression to obtain $(\hat{\sigma}_0, \hat{\sigma}_1, \dots, \hat{\sigma}_k)$.
- Step 4. Find μ_0, σ_0 and ξ that satisfy the following system of three equations under the condition that $(\hat{\mu}_1, \dots, \hat{\mu}_k)$ and $(\hat{\sigma}_1, \dots, \hat{\sigma}_k)$ are fixed:

$$\lambda_1 = l_1(\tilde{Z}_X), \quad \lambda_2 = l_2(\tilde{Z}_X), \quad \tau_3 = t_3(\tilde{Z}_X), \quad (20)$$

where λ_1, λ_2 , and τ_3 are the L-moments of a standard Gumbel distribution, and $l_1(\tilde{Z}_X), l_2(\tilde{Z}_X)$, and $t_3(\tilde{Z}_X)$ are sample L-moments calculated from the transformed data $\{\tilde{Z}_X\}$.

In Steps 1 to 3 of the above algorithm, we followed the WLS method by Strupczewski and Kaczmarek (2001) and Strupczewski et al. (2016), except for the robust regression in Step 1. The pseudo-residuals Q_t^{max} in Step 5 of the GN16 method are no longer employed. The transformation to $\{\tilde{Z}_X\}$ in Step 4 is a function of μ_0, σ_0 and ξ ; that is, $\tilde{Z}_X = \tilde{Z}_X\{\mu_0, \sigma_0, \xi \mid (\hat{\mu}_1, \dots, \hat{\mu}_k), (\hat{\sigma}_1, \dots, \hat{\sigma}_k)\}$. To solve a system of three equations in Step 4, we employed an iterative root-finding routine using the ‘nleqslv’ package (Dennis and Schnabel 1996) in R.

6.2 Model selection using cross-validated L-moment distance

Because we use L-moments in fitting NS GEV models, employing the likelihood-based criteria for the model selection does not seem appropriate. Thus, we consider a L-moment-based criterion for model selection, which is a cross-validated (CV) generalized L-moment distance (GLD).

For a given GEV model with parameter estimates, data can be transformed to $\{\tilde{Z}_X\}$ which may follow a standard Gumbel. Let denote

$$\underline{\lambda} = (\lambda_1, \lambda_2, \tau_3, \tau_4)^t \quad \text{and} \quad \underline{\mathbf{l}} = (l_1(\tilde{Z}_X), l_2(\tilde{Z}_X), t_3(\tilde{Z}_X), t_4(\tilde{Z}_X))^t \quad (21)$$

are vectors of the population L-moments of a standard Gumbel and sample L-moments of $\{\tilde{Z}_X\}$. The GLD is defined as

$$GLD = (\underline{\lambda} - \mathbf{1})^t V^{-1}(\underline{\lambda} - \mathbf{1}), \quad (22)$$

where V is the 4×4 variance-covariance matrix of the sample L-moments of $\{\tilde{Z}_X\}$. Here, V can be calculated using the formula by Elamir and Seheult (2004). The GLD has been used by Kjeldsen and Prosdocimi (2015) and Shin et al. (2025) for regional frequency analysis and model averaging, respectively.

For model selection purpose, the CV criteria have been widely employed (e.g., Smyth 2001; James et al. 2021; Stein 2021; Fauer and Rust 2023), because it is suitable to find a good model preventing the overfitting. Thus, we also applied the cross-validation idea to the GLD, for selecting the best model among the candidate NS GEV models which were built by the L-moment method. Because L-moments are less sensitive to outliers, we expect that the CV GLD is robust to outliers. To the best of our knowledge, the CV GLD has not been considered in the literature yet.

6.3 Application to maximum sea-levels in Fremantle

For a real data application of the NS GEV model with a physical covariate, we considered the annual maximum sea level (unit: meters) series recorded at Fremantle, West Australia. These data were analyzed by Coles (2001) and available from the ‘isnev’ package of R. The dataset consists of 86 observations from 1897 to 1989, spanning 93 years, with some missing data.

Coles (2001) fitted three NS GEV models with the following location parameters to these data using MLE with the Southern Oscillation Index (SOI) and time variables, with constant scale and shape parameters:

$$\begin{aligned} \text{Model 1 : } \mu(X) &= \mu_0 + \mu_1 \times t, \\ \text{Model 2 : } \mu(X) &= \mu_0 + \mu_1 \times SOI(t), \\ \text{Model 3 : } \mu(X) &= \mu_0 + \mu_1 \times t + \mu_2 \times SOI(t), \end{aligned} \quad (23)$$

where t denotes the index for the year, with $t = 1$ corresponding to 1897. Even though there are the missing data, t spans from 1 to 93.

We fitted the above three models to the Fremantle data using our algorithm. Table 6 provides the parameter estimates with SEs in parenthesis and the CV GLD values. The LME result from the stationary GEV model (Model 0) and MLE results from the Model 1 provided in Coles (2001) are presented for comparison. We applied the parametric bootstrap technique to compute the SEs of parameter estimates, as following;

- Step 1. Generate B bootstrap samples from the standard Gumbel distribution. Denote \tilde{Z}_X be the bootstrap sample.

- Step 2. Transform \tilde{Z}_X to obtain Z_X using

$$Z_X = \frac{\hat{\sigma}(X)}{-\hat{\xi}(X)} \exp\{-\hat{\xi}(X) \tilde{Z}_X\} + \hat{\mu}(X), \quad (24)$$

which is the back-transformation of (13).

- Step 3. Fit the NS GEV model for Z_X using considered methods.
- Step 4. Repeat Steps 2 and 3 for B bootstrap samples to compute the SEs of parameter estimates.

In this study, B was set to 300.

For calculating CV GLD, we used 20 times 5-fold cross-validation. The training and test data are randomly selected and fixed for each time. The covariance matrix was obtained after pooling the transformed full data from four models (Model 0 to 3) and was fixed throughout all the CV GLD computation.

In Table 6, the estimates and SEs in Model 1 are similar to those of the MLEs. Standard errors of $\hat{\mu}_1$ for the time t are smaller than those for variable SOI. This may be mainly due to the unit difference between the time t and SOI. The coefficients of variation ($\text{SE}/\hat{\mu}_1$) of $\hat{\mu}_1$ for the time t are 0.316, 0.25, and 0.3 for Model 1, Model 1*, and Model 3, respectively. Whereas the coefficients of variation of $\hat{\mu}_1$ for SOI are 0.367 and 0.328 for Model 2 and Model 3, respectively. The differences between coefficients of variation for the time t and SOI are not so remarkable. The similar argument using the coefficient of variation can be applied for comparison to SEs of other parameters. Finally, the Model 3 is selected as an appropriate model because of the smallest CV GLD, which is consistent with the model selection based on the likelihood tests in Coles (2001).

Table 6: The parameter estimates with standard errors in parenthesis and the cross-validated generalized L-moment distance (CV GLD) values for four models obtained by the L-moment-based method.

Model	$\hat{\mu}_0$	$\hat{\mu}_1$	$\hat{\mu}_2$	$\hat{\sigma}$	$\hat{\xi}$	CV GLD
Model 0 (Sta)	1.48 (.017)			.139 (.013)	.196 (.084)	16.70
Model 1 (t)	1.39 (.037)	.0019 (.0006)		.125 (.010)	.120 (.085)	15.95
Model 1 (t)*	1.38 (.03)	.0020 (.0005)		.124 (.010)	.125 (.070)	
Model 2 (SOI)	1.49 (.018)	.060 (.022)		.137 (.012)	.246 (.081)	16.43
Model 3 (t+SOI)	1.34 (.033)	.0020 (.0006)	.064 (.021)	.122 (.010)	.169 (.075)	15.54

*: Results using the maximum likelihood estimation provided by Coles (2001). Model 0: Stationary generalized extreme value model with L-moment estimates.

7 Discussion

In the simulation study, we observed that the MLE generally performed well, except for a few unusual samples, as depicted in the sample plots in the Supplementary Information. In these cases, MLE is heavily influenced by outliers or large values near the end of the sample, resulting in inferior performance, especially for $\xi \leq -0.2$. Therefore, a robust MLE method (e.g., Wilcox 2021; Grego and Yates 2024) or a penalized MLE approach (Cannon 2010; Papukdee et al. 2022) could mitigate this problem. We defer this investigation to future research endeavors.

In solving a system of three equations in Step 2 of the proposed method, we encountered a very few case where the proposed method produced nonunique solutions in the root-finding algorithm. To address this problem, we selected one solution with a minimum value of χ :

$$\chi = \sum_{i=T_1}^{T_{max}} \frac{|E_n(i) - S_n(i)|}{E_n(i)}, \quad (25)$$

where $T = (5, 10, 20, 40, T_{max})$, $E_n(i) = n/T_i$, and $S_n(i) = \sum_{j=1}^n I(x_j \geq q(T_i))$. Here, I is the indicator function where $I(A) = 1$ or $I(A) = 0$ if A is satisfied or not satisfied, respectively. Moreover, $q(T_i)$ is the RL corresponding to the return period T_i , calculated under the assumed model. In this study, we set $T_{max} = 80$ when $n = 50$. Further, $E_n(i)$ and $S_n(i)$ represent the expected number of observations that are greater than the RL corresponding to T_i without assuming any model and with the assumed model, respectively. Thus, the value in (25) serves as a distance measure for the expected number of events between the observations and the assumed model.

As with the transformation (13) to a standard Gumbel distribution in Step 2 of the proposed method, a similar transformation to the standard exponential distribution is available for the NS generalized Pareto model. Therefore, the proposed method for any NS model may be applicable whenever such a transformation to stationary sequences is available. However, Gumbel's choice is arguably the most natural, given its status within the GEV family (Coles 2001, pp. 111). Nonetheless, one can choose a unit Fréchet transformation: $Z_t^* = -1/\log \hat{F}_t(Z_t)$, where \hat{F}_t is the estimated CDF of the NS GEV model. However, Z_t^* still depends on the estimated shape parameter $\hat{\xi}$; thus, we hardly obtain the solution of a system of equations (14) without fixing $\hat{\xi}$. Therefore, we conclude that the unit Fréchet transformation is unsuitable for the proposed algorithm.

Motivated by Jan et al. (2021), we applied trimmed L-moments (Elamir and Scheult 2003) to the proposed method. However, the results of the limited simulation experiment using the trimmed L-moments did not exhibit significant improvement over the proposed method without trimming. Nevertheless, a trimmed L-moment approach can be helpful for samples with outliers.

8 Conclusion

Extreme values are inherently rare events, necessitating an effective method for fitting models using a few extreme observations. The L-moment method is more efficient than the MLE method for small samples. Therefore, this study proposed a method combining robust regression and L-moments to fit NS GEV models to time-series data. The proposed method improved the NS GEV model by addressing a weakness of the GN16 method, particularly regarding the GEV11 model with increasing variance. To illustrate the usefulness of the proposed method, we provided a real application using the extreme streamflow data from Trehafod in the UK. We extended the proposed method to an NS GEV model with physical covariates. Furthermore, we considered a model selection criterion based on the cross-validated generalized L-moment distance as an alternative to the likelihood-based criteria.

The likelihood-based method is often straightforward to apply in complex situations. In contrast, the L-moment-based method is not as straightforward. Thus, establishing an L-moment-based procedure for complex situations is challenging because the L-moment method is more efficient than the MLE method for small samples (of extreme values). This study is meaningful in that we considered developing a new methodology based on L-moments to build improved NS extreme value models.

Appendix

Estimation of each parameter in the WLS method

For further analysis from the WLS method, such as for calculating the standard error or for testing hypothesis on each parameter, we must obtain the final estimates for each parameter. In GEV11 model, we denote the final estimates as $\hat{\mu}_0^f$, $\hat{\mu}_1^f$, $\hat{\sigma}_0^f$, $\hat{\sigma}_1^f$, $\hat{\xi}^f$. To obtain these final estimates, we set the right-hand side of (9) to be the same as the effective RL (6). Then, by solving this equation with respect to the five parameters, we have the following:

$$\hat{\sigma}_0^f = \hat{\sigma}_0 + \log \hat{\sigma}_{st}, \quad \hat{\sigma}_1^f = \hat{\sigma}_1, \quad \hat{\xi}^f = \hat{\xi}_{st}. \quad (26)$$

However, $\hat{\mu}_0^f$ and $\hat{\mu}_1^f$ are not directly obtained because

$$\hat{\mu}_0^f + \hat{\mu}_1^f \times t = \hat{\mu}_0 + \hat{\mu}_1 \times t + \hat{\mu}_{st} \times \exp(\hat{\sigma}_0 + \hat{\sigma}_1 \times t). \quad (27)$$

To obtain approximated values of $\hat{\mu}_0^f$ and $\hat{\mu}_1^f$ in this study, we fitted the right-hand side of (27) to the simple regression for the time variable over the range $t = 1, 2, \dots, n$. Then, the estimated regression coefficients are approximated values of $\hat{\mu}_0^f$ and $\hat{\mu}_1^f$.

However, for some purposes such as computing T-year return level in (6) or (7), one can use the right-hand side of (27) directly as μ_t , instead of this approximation. Denote $\hat{\mu}_t^f$, $\hat{\sigma}_t^f$, $\hat{\xi}^f$

be the final estimates of NS parameters of GEV(μ_t, σ_t, ξ_t). Then

$$\hat{\mu}_t^f = \hat{\mu}_0 + \hat{\mu}_1 \times t + \hat{\mu}_{st} \times \exp(\hat{\sigma}_0 + \hat{\sigma}_1 \times t), \quad (28)$$

$$\hat{\sigma}_t^f = \exp(\hat{\sigma}_0 + \log \hat{\sigma}_{st} + \hat{\sigma}_1 \times t), \quad \hat{\xi}^f = \hat{\xi}_{st}. \quad (29)$$

Then we apply these estimates directly to (6) or (7).

For the GEV10 and GEV20 models, to obtain the final WLS estimates, we set the right-hand side of (9) to be the same as the effective RL (6). Then, by solving this equation with respect to the parameters, we obtain the final WLS estimates for the GEV10 model:

$$\hat{\mu}_0^f = \hat{\mu}_0 + \hat{\mu}_{st} \times \hat{\sigma}, \quad \hat{\mu}_1^f = \hat{\mu}_1, \quad \hat{\sigma}^f = \hat{\sigma} \times \hat{\sigma}_{st}, \quad \hat{\xi}^f = \hat{\xi}_{st}. \quad (30)$$

For the GEV20 model, we obtain the final WLS estimate $\hat{\mu}_2^f = \hat{\mu}_2$, while other parameters are the same as in (30).

Funding and acknowledgments

The authors thank the reviewers and the associate editor for their valuable comments and constructive suggestions that considerably improved the manuscript. This work was supported by the NRF grant (RS-2023-00248434) funded by the National Research Foundation of Korea and by Global - Learning & Academic research institution for Master's, PhD students, and Postdocs(LAMP) Program of National Research Foundation of Korea(NRF) grant funded by Ministry of Education (No. RS-2024-00442775).

Code and data availability

Peak streamflow data in Trehafod, UK: <https://nrfa.ceh.ac.uk/peak-flow-dataset>.

R code: https://github.com/yire-shin/non_stationary-gev.git

Conflict of interest

The authors declare no potential conflicts of interest.

ORCID

Yire Shin, 0000-0003-1297-5430; Yonggwon Shin, 0000-0001-6966-6511

Jeong-Soo Park, 0000-0002-8460-4869

Author contributions statement

Yire Shin and Jeong-Soo Park conceived the study, Yonggwon Shin conducted the analysis. All authors wrote the first draft, reviewed, edited, and approved the final manuscript.

References

AghaKouchak A, Easterling D, Hsu K, Schubert S, Sorooshian S (Eds.) 2013. *Extremes in a changing climate: Detection, analysis and uncertainty*. Springer.

- Asquith WH (2011) *Distributional analysis with L-moment statistics using the R environment for statistical computing*, First ed. CreateSpace. Available from <http://www.amazon.com>
- Baldan D, Coraci E, Crosato F, Ferla M et al.(2022) Importance of non-stationary analysis for assessing extreme sea levels under sea level rise. *Nat Hazards Earth Syst Sci*, 22:3663–3677.
- Bousquet N, Bernardara P (Eds.) (2021) *Extreme value theory with applications to natural hazards*, Springer.
- Choi G (2021) A new approach for detecting gradual changes in non-stationary time series with seasonal effects. *J. Korean Stat. Soc.* 50, 419–430.
- Cannon AJ (2010) A flexible nonlinear modelling framework for nonstationary generalized extreme value analysis in hydroclimatology. *Hydro Process*, 24:673–685.
- Coles S (2001) *An introduction to statistical modeling of extreme values*. Springer, London.
- Cooley D (2013) Return periods and return levels under climate change, in AghaKouchak A, Easterling D et al. (Eds.):*Extremes in a changing climate: Detection, analysis and uncertainty*. Springer.
- Cunderlik JM, Burn DH (2003) Non-stationary pooled flood frequency analysis. *J Hydro* 276:210-223.
- Dennis, J.E. Jr and Schnabel, R.B. (1996), *Numerical Methods for Unconstrained Optimization and Nonlinear Equations*, SIAM, Philadelphia.
- Elamir EAH, Scheult AH (2003) Trimmed L-moments. *Comput Stat Data Anal* 43:299-314.
- Elamir EA, Scheult AH (2004) Exact variance structure of sample L-moments. *Jour Statist Plann Infer* 124(2):337-359.
- Fauer, F.S., Rust, H.W. (2023) Non-stationary large-scale statistics of precipitation extremes in central Europe. *Stoch Environ Res Risk Assess* 37, 4417–4429.
- Gado TA, Nguyen VTN (2016a) An at-site flood estimation method in the context of nonstationarity I. A simulation study. *J Hydro* 535:710-721.
- Gado TA, Nguyen VTN (2016b) An at-site flood estimation method in the context of nonstationarity II. Statistical analysis of floods in Quebec. *J Hydro* 535:722-736.
- Grego JM, Yates PA (2024). Robust Local Likelihood Estimation for Non-stationary Flood Frequency Analysis. *J Agri Bio Envir Stat*, 1-20. <https://doi.org/10.1007/s13253-024-00614-0>
- Hosking JRM (1990) L-Moments: Analysis and Estimation of Distributions Using Linear Combinations of Order Statistics. *J Royal Stat Soc B*, 52(1):105-124
- Hosking JRM, Wallis JR, Wood EF (1985) Estimation of the generalized extreme-value distribution by the method of probability weighted moments. *Technometrics*, 27:251-261.
- Hosking JRM, Wallis JR (1997) *Regional Frequency Analysis: An Approach Based on L-Moments*. Cambridge Univ Press, Cambridge.
- Hossain, I., Imteaz, M.A. & Khastagir, A (2021) Effects of estimation techniques on generalised extreme value distribution (GEVD) parameters and their spatio-temporal variations. *Stoch Environ Res Risk Assess* 35, 2303–2312.
- Jeong BY, Murshed MS, Seo YA, Park J-S (2014) A three-parameter kappa distribution with hydrologic application: A generalized Gumbel distribution. *Stoch Environ Res Risk Assess* 28(8):2063-2074.
- James G, Witten D, Hastie T, Tibshirani R (2021) *An Introduction to Statistical Learning: With Applications in R*, 2nd ed. Springer.
- Jan NAM, Shabri A, Samsudin R (2020) Handling non-stationary flood frequency analysis using TL-moments approach for estimating parameter. *J Water Clim Change*, 11(4):966-979.

- Katz R (2013) Statistical methods for nonstationary extremes, in AghaKouchak, A., Easterling, D. et al.(Eds.) *Extremes in a changing climate: Detection, analysis and uncertainty*, Springer.
- Kjeldsen T.R., Prosdocimi I.(2015) A bivariate extension of the Hosking and Wallis goodness-of-fit measure for regional distributions. *Water Resour Res.* 51(2), 896-907.
- Koller M, Stahel WA (2017) Nonsingular subsampling for regression S estimators with categorical predictors, *Comput Stat* 32(2):631–646.
- Konzen E, Neves C, Jonathan P (2021) Modeling nonstationary extremes of storm severity: Comparing parametric and semiparametric inference. *Environmetrics* 32(4):e2667.
- Mudersbach C. and Jensen J (2010) Nonstationary extreme value analysis of annual maximum water levels for designing coastal structures on the German North Sea coastline, *J Flood Risk Manag* 3:52-62.
- Naghattini M (ed)(2017) *Fundamentals of Statistical Hydrology*. Springer.
- Olsen J, Lambert JH, Haines T (1998) Risk of extreme events under nonstationary conditions. *Risk Anal* 18:497-510.
- Papukdee N, Park J-S, Busababodhin P (2022) Penalized likelihood approach for the four-parameter kappa distribution. *Jour Appl Stat*, 49(6):1559-1573.
- Parey S, Hoang TTH, Dacunha-Castelle D (2010) Different ways to compute temperature return levels in the climate change context. *Environmetrics* 21:698-718.
- Parey S, Hoang TTH (2021) Extreme values of non-stationary time series, in Bousquet N, Bernardara P (Eds) *Extreme value theory with applications to natural hazards*, Springer.
- Prahadchai T, Shin Y, Busababodhin P, Park J-S (2023) Analysis of maximum precipitation in Thailand using non-stationary extreme value models. *Atmos Sci Lett*, 24(4), e1145.
- Radfar S, Galiatsatou P, Wahl T (2023) Application of nonstationary extreme value analysis in the coastal environment – A systematic literature review. *Weath Clim Extrem*, 41, 100575.
- Reiss R-D, Thomas M (2007) *Statistical analysis of extreme values*, 3rd ed. Birkhauser.
- Ribereau P, Guillou A, Naveau P (2008) Estimating return levels from maxima of non-stationary random sequences using the generalized PWM method. *Nonlin Process Geophys*, 15:1033-1039.
- Salas JD, Obeysekera J (2014) Revisiting the concepts of return period and risk for nonstationary hydrologic extreme events. *J Hydro Eng*, 19:554–568.
- Salas JD, Obeysekera J, Vogel RM (2018) Techniques for assessing water infrastructure for nonstationary extreme events: A review. *Hydrol Sci J* 63(3):325-352.
- Shin Y, Shin Y, Park J-S (2025) Model averaging with mixed criteria for estimating high quantiles of extreme values: Application to heavy rainfall. Preprint at <http://arxiv.org/abs/2505.21417>
- Smyth, P (2000) Model selection for probabilistic clustering using cross-validated likelihood. *Stat and Comput* 10, 63–72.
- Stein ML (2021) A parametric model for distributions with flexible behavior in both tails, *Environmetrics* 32(2), e2658.
- Strupczewski WG, Kaczmarek Z (2001) Non-stationary approach to at-site flood frequency modelling. Part II. Weighted least squares estimation. *J Hydro*, 48(14):143-151.
- Strupczewski WG, Kochanek K, Bogdanowicz E, et al. (2016) Comparison of two nonstationary flood frequency analysis methods within the context of the variable regime in the representative Polish rivers, *Acta Geophysica*, 64(1):206-236.
- Wilcox RR (2021) *Introduction to robust estimation and hypothesis testing*, 5th Ed. Academic Press.

Yilmaz A, Kara M, Özdemir O (2021) Comparison of different estimation methods for extreme value distribution. *J Appl Stat*, 48(13-15):2259-2284.

Yohai V.J. (1987) High breakdown point and high efficiency robust estimates for regression. *Ann Stat* 15:642-656.